JOURNAL OF VIROLOGY, Apr. 2007, p. 3545–3553 Vol. 81, No. 7
0022-538X/07/$08.00+0 doi:10.1128/JVI.01080-06

Expression of Rotavirus NSP4 Alters the Actin Network Organization through the Actin Remodeling Protein Cofilin▽

Zuzana Berkova,[1,2] Sue E. Crawford,[1] Sarah E. Blutt,[1] Andrew P. Morris,[2]* and Mary K. Estes[1]*

Baylor College of Medicine, Department of Molecular Virology and Microbiology, One Baylor Plaza,[1] and University of Texas, Health Science Center, Department of Integrative Biology and Pharmacology, 6341 Fannin,[2] Houston, Texas 77030

Received 25 May 2006/Accepted 19 December 2006

Rotavirus is a major cause of infantile gastroenteritis with a multifactorial pathogenesis. As with many other pathogens, rotavirus infection and replication leads to rearrangement of the cytoskeleton with disorganization of cytoskeletal elements such as actin and cytokeratin through a calcium-dependent process that has not been fully characterized. The rotavirus enterotoxin NSP4, shown previously to elevate intracellular calcium levels when added exogenously as well as when expressed intracellularly, is a key player in intracellular calcium regulation during rotavirus infection. Here, we investigated the role NSP4 may play in actin rearrangement. Expression of NSP4 fused to enhanced green fluorescent protein (NSP4-EGFP), but not expression of EGFP alone, caused stabilization of long cellular projections in fully confluent HEK 293 cells. Cells expressing NSP4-EGFP for 24 h were also resistant to cell rounding induced by cytochalasin D. Quantification of filamentous actin (F-actin) content by using rhodamine-conjugated phalloidin and flow cytometry showed an elevated F-actin content in NSP4-EGFP-expressing and rotavirus-infected cells in comparison with that in nonexpressing and noninfected cells. Normalization of intracellular calcium levels prevented alterations of F-actin content. Observed changes in F-actin amounts correlated with the increased activation of the actin-remodeling protein cofilin. These calcium-dependent actin rearrangements induced by intracellular NSP4 expression may contribute to rotavirus pathogenesis by interfering with cellular processes dependent on subcortical actin remodeling, including ion transport and viral release.

Rotavirus is a major cause of infantile diarrhea worldwide, claiming approximately 600,000 lives annually (40). The pathogenesis of rotavirus is not yet fully understood, but the involvement of multiple signaling pathways has been suggested. It was shown 30 years ago that rotavirus infects mature enterocytes in the upper villi in the small intestine of the host (16, 25). However, rotavirus tissue tropism is not necessarily restricted to the gut. In tissue culture cells, rotavirus replicates in many cell types (epithelial as well as nonepithelial), and recent data show extraintestinal spread of rotavirus in infected children and animals (2, 7, 8, 15, 21, 34, 35, 50). In polarized human intestinal Caco-2 cells, rotavirus infection induces calcium-dependent depolymerization of microvillar actin and interferes with protein trafficking (9, 27) and cell monolayer integrity by disruption of tight junctions (39). Brunet et al. (9) showed that a viral protein secreted into the medium of infected Caco-2 cells likewise causes disassembly of microvillar actin in noninfected cells. The best candidate for this extracellular activity is the rotavirus enterotoxin NSP4, shown to be secreted into the medium of rotavirus-infected cells (49). When added to the apical media of polarized MDCK-1 cells, NSP4 causes filamentous actin (F-actin) redistribution accompanied by a reduction of transepithelial resistance (44). Extracellular NSP4 (eNSP4) affects intracellular calcium levels through activation of phospholipase C (PLC) (18). This suggests a role for eNSP4 in actin cytoskeleton changes via PLC signaling. However, a second, PLC-independent mode of intracellular calcium elevation is also recognized for intracellular NSP4 (iNSP4) (6).

In this study, we investigated the effects of iNSP4 expression and thus the effects of chronic, PLC-independent elevation of intracellular calcium levels on cell structure. To minimize the cytotoxicity of NSP4 expression (45), we used an inducible HEK 293-derived cell line that expresses NSP4 fused to enhanced green fluorescent protein (EGFP) upon activation of a tetracycline (Tet)-responsive promoter (5, 6). Striking changes observed in confluent cells expressing NSP4-EGFP were (i) the presence of long cellular projections, (ii) partial resistance to cytochalasin D-induced cell rounding, and (iii) increased F-actin content. This paper reports studies aimed at understanding the molecular basis of these changes. We found that intracellularly expressed NSP4 causes sub-plasma membrane actin reorganization in a calcium-dependent manner through decreased phosphorylation of the actin remodeling protein cofilin.

MATERIALS AND METHODS

Cell culture. The previously described (5, 6) HEK 293 "Tet-on" cells inducibly expressing NSP4-EGFP (HEK 293/NSP4-EGFP cells) were maintained according to recommendations from Clontech Laboratories, Inc. Briefly, cells were kept at 37°C under 5% CO_2 in minimal essential medium (MEM) with alpha modification (Sigma-Aldrich Co., St. Louis, MO), with 10% Tet system-approved fetal bovine serum (FBS; Clontech Laboratories, Inc., Palo Alto, CA), 2 mM L-glutamine (Sigma-Aldrich Co., St. Louis, MO), 100 μg/ml Geneticin, and 37.5 μg/ml hygromycin B (both from Gibco BRL, Life Technologies, Inc., Gaithersburg, MD). Cells were split at a ratio of 1:3 twice per week. The HEK 293 cells were maintained under identical conditions with omission of Geneticin and hygromycin B. The MA104 cells were grown at 37°C under 5% CO_2 in high-

* Corresponding author. Mailing address for Mary K. Estes: Baylor College of Medicine, Department of Molecular Virology and Microbiology, 1200 Moursund St., Houston, TX 77030-3404. Phone: (713) 798-3585. Fax: (713) 798-3586. E-mail: mestes@bcm.edu. Mailing address for Andrew P. Morris: University of Texas, Health Science Center, Department of Integrative Biology and Pharmacology, 6341 Fannin, Houston, TX 77030. Phone: (713) 500-6681. Fax: (713) 500-7444. E-mail: Andrew.P.Morris@uth.tmc.edu.

▽ Published ahead of print on 17 January 2007.

glucose Dulbecco's MEM (DMEM) (Gibco BRL, Life Technologies, Inc., Gaithersburg, MD) supplemented with 10% FBS.

Transfections/virus infections. HEK 293 and MA104 cells were seeded into 6-well plates and grown at 37°C under 5% CO_2 as described above. Cells were transfected with 1.5 μg of p-EGFP-N1 (Clontech Laboratories, Inc., Palo Alto, CA) or 4 μg of p-EGFP-NSP4 plasmids (5, 6) using Lipofectamine 2000 (Gibco BRL, Life Technologies, Inc., Gaithersburg, MD) according to the manufacturer's recommendations. The lower concentration of the p-EGFP-N1 plasmid was used to decrease the number of EGFP-expressing cells in order to allow us to visualize cell shape in confluent cells.

For small interfering RNA (siRNA) experiments, MA104 cells seeded in six-well plates were grown to ~70% confluence. The cells were washed in serum-free medium, and a mixture of 75 pmol of annealed duplex siRNA (Dharmacon Research, Lafayette, CO) (rhesus rotavirus [RRV] NSP4 siRNA sequence, AA GGCCUCGGUUCCAACCAUG [31]; SA11 clone 3 siRNA sequence, AAGC CACAGUCAGCCAUAUCG; Norwalk virus ORF3 siRNA sequence, AAGCG GCCCUCCAAAGCCAAA) and 9.5 μl of Lipofectamine 2000 (Invitrogen), or the lipid mixture without siRNA, in 500 μl OptiMEM, was added to each well. After 4 to 5 h of incubation, 2 ml of DMEM containing 10% FBS was added to each well. Transfected cells were infected 72 h after transfection with either RRV or SA11 clone 3 rotavirus or mock infected.

For virus infections, serum-free medium was put on the cells 1 h before infection. Rotavirus simian strains SA11 and RRV, and human strain PA169, diluted in serum-free medium, were inoculated onto cells for 1 h at 37°C at a multiplicity of infection of 3 or 10. Upon removal of the inoculum, cells were grown in serum-free regular DMEM or DMEM supplemented with 2 mM EGTA. Cells were harvested 7 and 18 h postinfection and analyzed by Western blotting or by flow cytometry.

Immunofluorescence and confocal microscopy. Cells were seeded onto 4-chamber microscope slides (2×10^4 cells/chamber) and induced with 10 μg/ml doxycycline for 1.5 h. The doxycycline-containing medium was then replaced with a regular culture medium (without doxycycline). Cytochalasin D was added to the medium where indicated at a 1 μM final concentration (24). Twenty-four hours postinduction, cells were fixed with 4% formaldehyde in 0.01 M phosphate-buffered saline (PBS) for 30 min at 4°C and permeabilized with 0.5% Triton X-100 for 30 min. After three washes with PBS, slides were incubated with 10 nM rhodamine-conjugated phalloidin (Molecular Probes, Eugene, OR) in PBS for 30 min at 4°C. Excess conjugated phalloidin was removed by three washes with PBS. Slides were then mounted with Vectashield mounting medium (Alexis PLATFORM, San Diego, CA).

Mounted slides were observed using a Zeiss LSM 510 META confocal microscope with a 63× immersion oil objective (Carl Zeiss, Germany) in multitrack mode with the excitation wavelengths set to 488 nm (argon laser) and 543 nm (HeNe laser) and the emission wavelengths set to 505 to 530 nm and >560 nm for EGFP and rhodamine signal detection, respectively. Single optical slices were set to 0.8 μM and Z-stack slices to 0.38 μM. Collected images were processed using LSM Image VisArt (Carl Zeiss, Inc., Thornwood, NY) and saved in a 12-bit tagged-image RGB format.

Flow cytometry analysis. HEK 293/NSP4-EGFP or MA104 cells were seeded on 6-well plates (1×10^6 cells/well) and induced with doxycycline or infected with rotavirus as described above. Twenty-four hours postinduction/18 h postinfection, cells were collected from each well by scraping and pipetting, followed by a slow-speed centrifugation (500 rpm for 10 min). HEK 293/NSP4-EGFP cells were fixed with 500 μl CytoFix/CytoPerm solution (Pharmingen, San Diego, CA) for 30 min at 4°C and subsequently washed three times with 1 ml of Perm/Wash buffer (Pharmingen, San Diego, CA). Washed cells were incubated with 500 μl of rhodamine-conjugated phalloidin for 30 min at 4°C. Rotavirus-infected MA104 cells were detached by a brief treatment with trypsin and collected in PBS. Cells were then fixed by addition of ice-cold methanol during vortexing and incubated for 15 min on ice. Upon removal of methanol, cells were washed with PBS and then incubated with a primary rabbit anti-rotavirus antibody for 1 h at room temperature (RT). The cells were washed in PBS and subsequently incubated with a fluorescein isothiocyanate (FITC)-conjugated mouse anti-rabbit secondary antibody (BD Pharmingen, San Jose, CA) and rhodamine-conjugated phalloidin as described above. After three washes, cells were suspended in 500 μl of 2% FBS in PBS and analyzed by Beckman-Coulter EPICS XL-MCL (Beckman-Coulter, Inc., Fullerton, CA) using FITC and phycoerythrin filters for detection of EGFP/FITC and rhodamine-phalloidin fluorescence, respectively.

Manipulation of intracellular calcium levels. The HEK 293/NSP4-EGFP cells were seeded and induced as described above or left uninduced. To lower intracellular calcium levels in NSP4-EGFP-expressing cells, cells were grown in MEM with alpha modification (Sigma-Aldrich Co., St. Louis, MO), supplemented with 10% Tet system-approved fetal bovine serum (Clontech Laboratories, Inc., Palo Alto, CA) and 2 mM EGTA, and analyzed 24 h postinduction. To increase intracellular calcium levels, cells were incubated for 8 h before analysis with 200 nM thapsigargin (Molecular Probes, Eugene, OR).

Measurement of intracellular calcium levels. The HEK 293/NSP4-EGFP cells were seeded onto poly-D-lysine (Sigma-Aldrich Co., St. Louis, MO)-coated coverslips. After a 1.5-h adherence/induction period, the seeding medium was replaced with doxycycline-free regular culture medium (as above). To lower intracellular calcium levels in NSP4-EGFP-expressing cells, MEM with alpha modification (Sigma-Aldrich Co., St. Louis, MO) supplemented with 10% Tet system-approved fetal bovine serum (Clontech Laboratories, Inc., Palo Alto, CA) and 2 mM EGTA was used. Twenty-four hours postinduction, coverslips were mounted on measurement chambers, and the cells were loaded for 60 min at 30°C with 8 μM Fura-2 in sodium HEPES buffer with or without 1 mM $CaCl_2$ for measurement of normal and lowered intracellular calcium levels, respectively. Fura-2-loaded cells were then continuously washed with sodium HEPES buffer (with or without 1 mM $CaCl_2$) for 20 min at 37°C to remove any extracellular dye. Cells were subjected to a dual-excitation, single-emission ratio imaging of intracellular calcium concentrations using a modified high-resolution camera/image-intensifier system as described previously (6, 33).

Western blotting. Cells were seeded onto tissue culture dishes, collected in PBS, and lysed in Laemmli buffer. Lysates were then boiled for 10 min and analyzed by electrophoresis on 15% sodium dodecyl sulfate-polyacrylamide gel electrophoresis (SDS-PAGE) gels. Separated proteins were then transferred from the gel to a nitrocellulose membrane (Amersham Biosciences, Piscataway, NJ). Membranes were blocked in 5% Blotto (5% fat-free Carnation milk in 0.01 M PBS) and incubated with a rabbit anti-NSP4, amino acids 120 to 147, anti-cofilin, anti-phosphocofilin antibody (Chemicon International, Inc., Temecula, CA), mouse monoclonal antibodies to glyceraldehyde-3-phosphate dehydrogenase (GAPDH), and actin (Chemicon International, Inc., Temecula, CA), all in 0.5% Blotto overnight at RT. Primary antibodies were removed, and membranes were washed three times with 0.5% Blotto. An alkaline phosphatase-conjugated secondary goat anti-rabbit immunoglobulin G antibody and a goat anti-mouse immunoglobulin G antibody (Sigma-Aldrich Co., St. Louis, MO) were incubated with the membranes for 4 h at RT and subsequently washed three times with 0.5% Blotto. Membranes were then developed with 5-bromo-4-chloro-3-indolylphosphate-*p*-nitroblue tetrazolium chloride substrate (Amersham Biosciences, Piscataway, NJ).

RESULTS

The actin network is altered in NSP4-EGFP-expressing cells. To study the effects of intracellular NSP4 expression, we constructed an NSP4-EGFP fusion protein and subsequently generated a HEK 293-based cell line inducibly expressing NSP4-EGFP (5, 6). An obvious difference observed by visual inspection of EGFP- and NSP4-EGFP-expressing cells was the presence of long cellular projections in NSP4-EGFP-expressing cells. This morphological phenotype was apparent in HEK 293 and MA104 cells transiently transfected with a pEGFP-NSP4 plasmid (Fig. 1), as well as in the induced HEK 293/NSP4-EGFP cells. Long projections are normally present in low-density HEK 293 cell cultures (Fig. 1A, B, and C) and reflect the processes of cell spreading and substratum adhesion (20) but are lost in high-density (confluent) cell layers (Fig. 1D and E) following the formation of cell-cell contacts and the physical constraints of cell packing. To quantify the differences between EGFP- and NSP4-EGFP-expressing cells, six random optical fields of confluent EGFP- and NSP4-EGFP-expressing cultures were analyzed for the number of cells with projections longer than the cell diameter. NSP4-EGFP expression correlated with a 5.1-fold increase in the number of cells with such projections compared to cells expressing EGFP alone ($P < 0.001$ by chi-square analysis). The continued presence of long projections in confluent HEK 293 and MA104 cell layers expressing NSP4-EGFP (Fig. 1F and H) suggested differences in cytoskeleton organization.

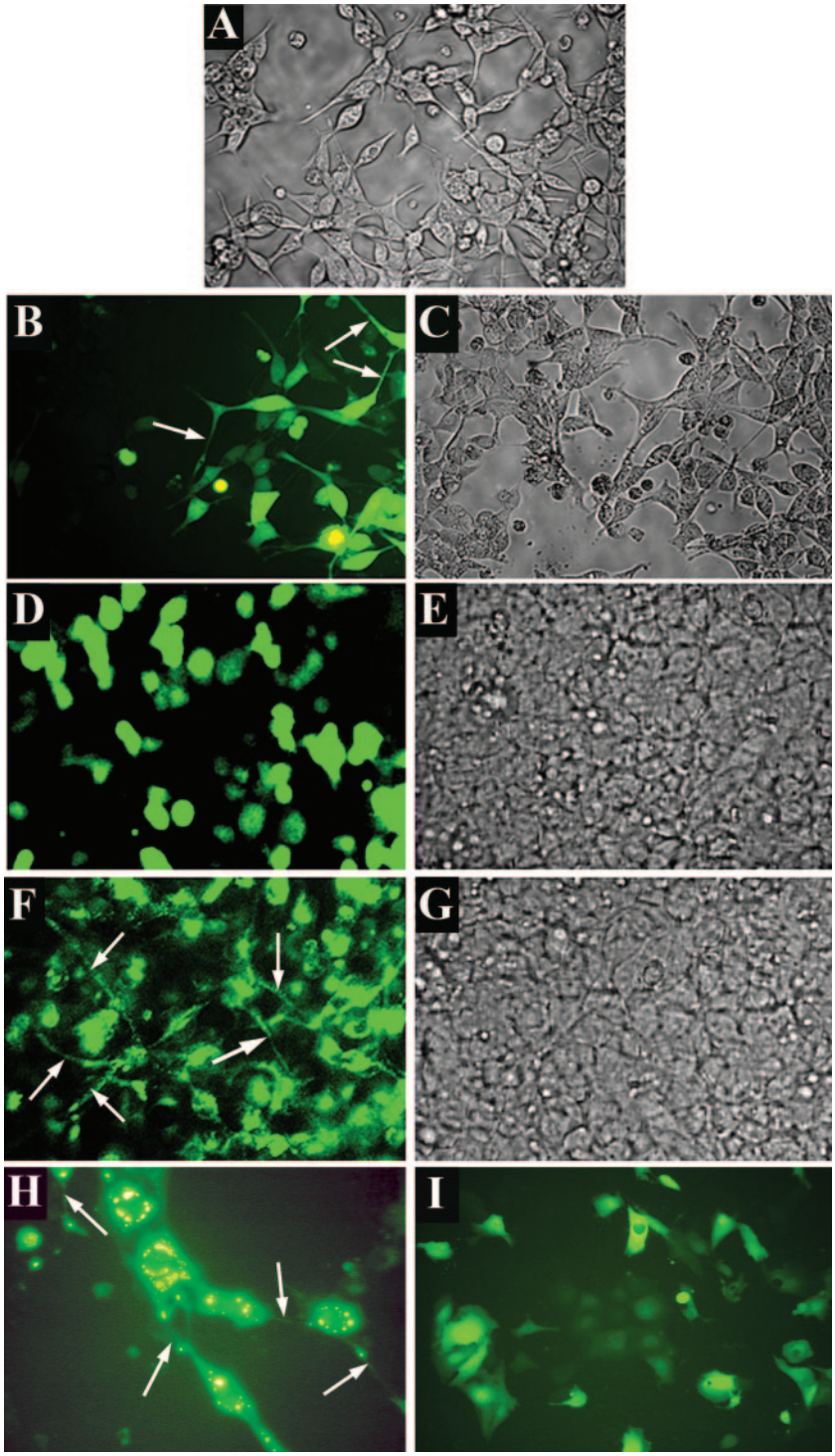

FIG. 1. NSP4-EGFP expression causes retention of long cellular projections in HEK 293 cells and MA104 cells. Cells were transfected with an EGFP- or NSP4-EGFP-expressing plasmid, and cell morphology was observed under white light (A, C, E, and G) or fluorescent light (B, D, F, H, and I) at ×20 magnification. (A) Low-density HEK 293 cell culture; (B and C) EGFP fluorescence and bright-field images of EGFP-expressing low-density HEK 293 cells 24 h posttransfection; (D and E) EGFP fluorescence and bright-field images of EGFP-expressing confluent HEK 293 cells 24 h posttransfection; (F and G) NSP4-EGFP fluorescence and bright-field images of NSP4-EGFP-expressing confluent HEK 293 cells 24 h posttransfection. (H) NSP4-EGFP fluorescence in MA104 cells; (I) EGFP fluorescence in MA104 cells. Arrows indicate long projections.

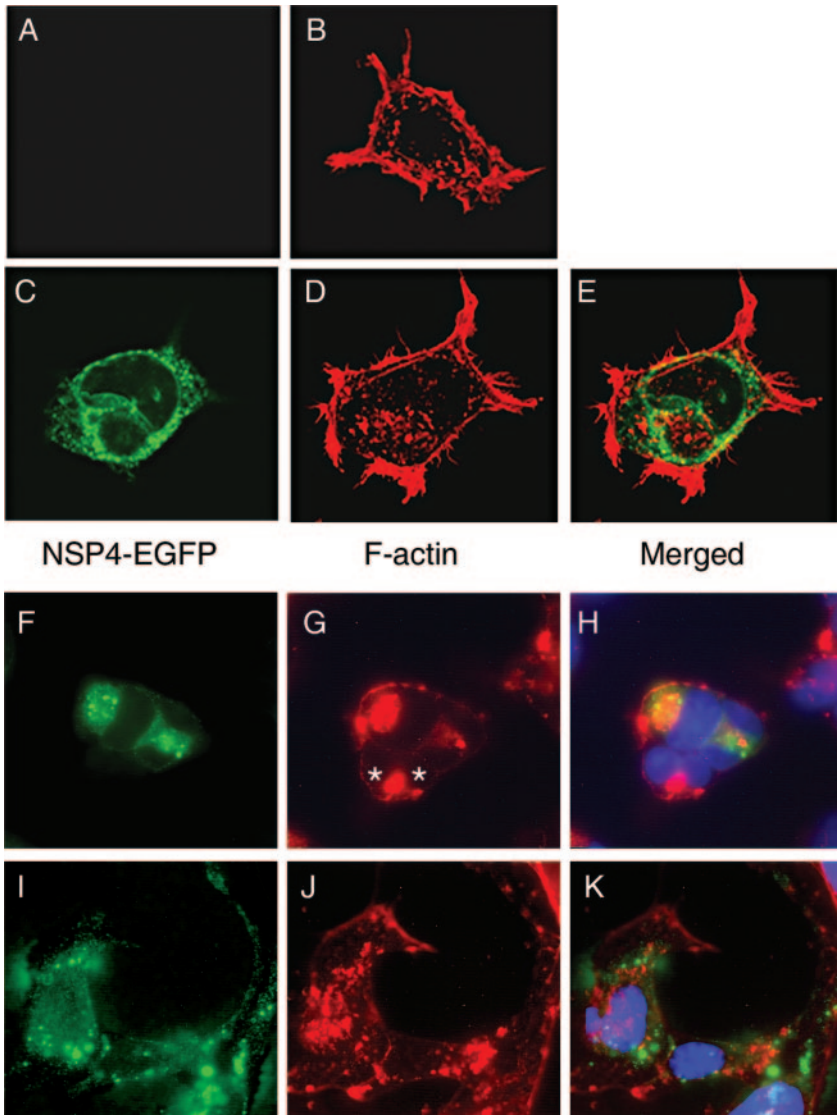

FIG. 2. NSP4-EGFP expression in HEK 293 cells increases F-actin staining and confers partial resistance to cytochalasin D. HEK 293/NSP4-EGFP cells were seeded and induced or left uninduced as control cells. At the indicated times, cells were incubated with 1 μM cytochalasin D and fixed. After fixation, cells were stained with rhodamine-conjugated phalloidin and Hoechst blue and were observed under a confocal microscope. (A and B) Uninduced HEK 293/NSP4-EGFP cells 24 h postseeding. (C, D, and E) Induced HEK 293/NSP4-EGFP cells 24 h after seeding and induction. (F, G, and H) Induced cells 24 h after induction with cytochalasin D treatment. (I, J, and K) Induced cells 48 h after induction with cytochalasin D treatment for the last 24 h. Green, NSP4-EGFP fluorescence; red, rhodamine-phalloidin-stained F-actin; blue, Hoechst blue. NSP4-EGFP-negative cells are asterisked (G).

The actin network is involved in the formation of cell protrusions (28). To look for possible modifications of the actin network in NSP4-EGFP-expressing cells, we took advantage of the specific binding of phalloidin to polymerized F-actin (14). The F-actin staining of uninduced and induced HEK 293/NSP4-EGFP cells with rhodamine-conjugated phalloidin revealed thick finger-like protrusions and overall higher peripheral (subcortical) cytoplasmic staining when NSP4-EGFP was expressed intracellularly (Fig. 2, panel B versus panel D). Treatment of induced cells with the actin network untethering agent cytochalasin D (14) from the time of doxycycline induction caused cell rounding and condensation of F-actin into the perinuclear region (Fig. 2F to H) irrespective of NSP4-EGFP expression (Fig. 2G). However, treatment of cells with cytochalasin D 24 h post-NSP4-EGFP induction failed to elicit similar morphological changes. Instead, NSP4-EGFP-expressing cells retained their irregular shape, projections were still visible, and dispersed F-actin foci were identified throughout the cytoplasm (Fig. 2I to K). This resistance to cytochalasin D-induced changes in cell shape indicated that expression of NSP4-EGFP affected the subcortical actin network via actin tethering and/or the stabilization of actin polymerization.

The amount of F-actin is elevated in NSP4-EGFP-expressing cells and rotavirus-infected cells. The presence of thicker and more frequent finger-like projections and overall higher subcortical F-actin staining in NSP4-EGFP-expressing cells

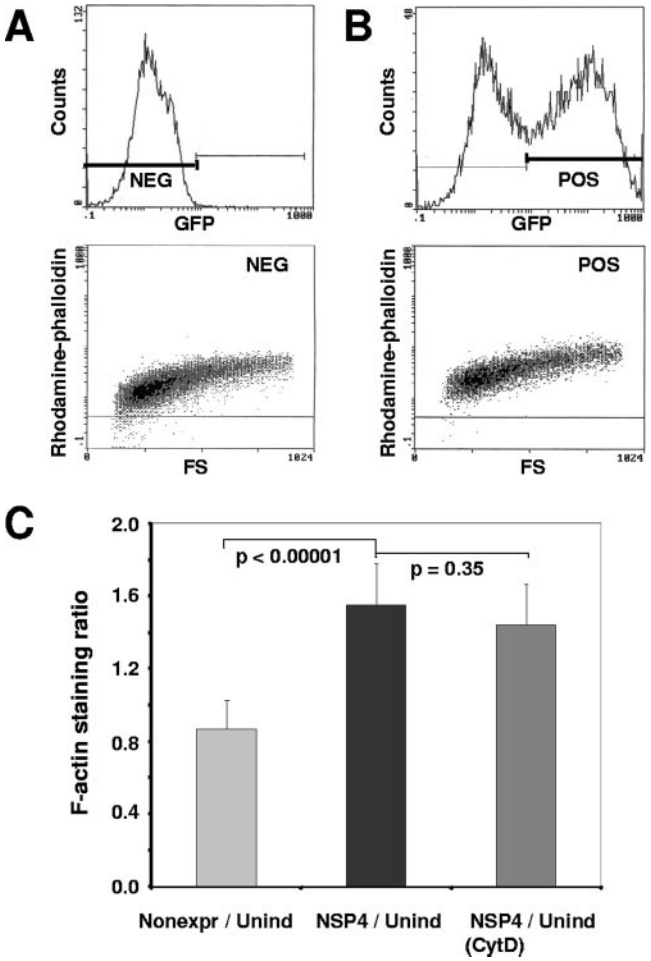

FIG. 3. NSP4-EGFP expression increases F-actin amounts in HEK 293 cells as detected by flow cytometry. Cells were seeded and induced or left uninduced as a control. Twenty-four hours after seeding/induction, cells were collected, lightly fixed, and stained with rhodamine-conjugated phalloidin. Labeled cells were then analyzed by flow cytometry for the intensity of EGFP and rhodamine fluorescence. (A) Uninduced cells. (Top) EGFP fluorescence intensity analysis. (Bottom) F-actin staining as the fluorescence intensity of rhodamine-conjugated phalloidin. (B) Induced cells. (Top) EGFP fluorescence intensity. (Bottom) F-actin staining as intensity of rhodamine-conjugated phalloidin in the EGFP-positive population. (C) Ratios of F-actin staining for induced nonexpressing cells versus uninduced control cells (light gray), induced NSP4-EGFP-expressing cells versus uninduced control cells (black), and induced NSP4-EGFP-expressing cells treated with cytochalasin D versus uninduced cells (gray). Data represent eight and six pairs of induced and uninduced cell populations in three separate experiments. *P* values were calculated using the Student *t* test.

(Fig. 2D and B, respectively) implied a possible increase in cellular F-actin content within NSP4-EGFP-expressing cells. To quantify the amount of F-actin in induced and uninduced cells, we analyzed rhodamine-conjugated phalloidin-stained cells by flow cytometry. The degree of phalloidin binding reflects the degree of cellular actin polymerization (14); thus, the fluorescence intensity correlates with the amount of F-actin within the cells. The quantitative cellular fluorescence output (gated at emission wavelengths of 525 ± 25 nm for EGFP-NSP4 and 580 ± 15 nm for rhodamine-phalloidin) of a representative pair of uninduced and induced cell populations is shown in Fig. 3A and B, respectively. Higher rhodamine-phalloidin intensity values corresponding to F-actin staining were observed in NSP4-EGFP-positive cell populations compared to uninduced cell populations (bottom panels of Fig. 3B and A, respectively), while comparable values of F-actin staining were detected in uninduced and induced nonexpressing cell populations (Fig. 3C). The mean (population-averaged) F-actin staining value of NSP4-EGFP-expressing cells (Fig. 3C) was approximately 1.5 times higher ($P < 0.0001$) than that of uninduced cells and 1.8 times higher than that recorded for the non-pair-matched, nonexpressing cells (data not shown), while there was no statistically significant difference between uninduced and nonexpressing cell populations. Cytochalasin D treatment of NSP4-EGFP-expressing cells failed to significantly affect the mean (population-averaged) F-actin staining value of induced cells (Fig. 3C) as well as uninduced controls (data not shown). This result is to be expected from the untethering properties of cytochalasin D (14).

We next determined if the increased F-actin content in NSP4-EGFP-expressing cells was also observed in rotavirus-infected cells. The F-actin content in rotavirus-infected MA104 cells (average rhodamine-phalloidin intensity value, 1.97 ± 0.34) versus mock-infected controls (1.34 ± 0.026) showed an F-actin ratio of 1.5. This ratio was identical to that observed for NSP4-EGFP-expressing cells versus nonexpressing cells, indicating that NSP4 expression alone or in the context of rotavirus-infected cells increased the cellular F-actin content.

Increased cellular F-actin content is dependent on NSP4-EGFP expression-induced increases in intracellular calcium levels. The results presented so far indicate that NSP4-EGFP cells contain larger amounts of F-actin and that their actin network is also more resistant to cytochalasin D-induced reorganization. In our previous work, we showed that HEK 293 cells inducibly expressing NSP4-EGFP have intracellular calcium levels more than twofold higher than those of uninduced control cells (6). This raised the question of whether the elevation of cellular F-actin content observed in NSP4-EGFP-expressing cells by flow cytometry was related to NSP4-induced changes in intracellular calcium concentrations. To address this question, doxycycline induced HEK 293/NSP4-EGFP-expressing cells were grown in calcium-free medium to normalize their intracellular calcium levels to values comparable with those recorded in nonexpressing cells (Fig. 4A) (5). Flow cytometry analysis showed that the population-averaged cellular F-actin content of NSP4-EGFP-expressing cells under these conditions fell to values comparable with those recorded in non-NSP4-EGFP-expressing cell populations maintained in regular culture medium (Fig. 4B). These results indicated that NSP4-EGFP-mediated changes in intracellular calcium signaling are involved in the elevation of F-actin content.

NSP4-EGFP-expressing cells have increased activation of cofilin. The immunofluorescence findings, which demonstrated that NSP4-EGFP failed to colocalize with actin into subcortical networks that line the finger-like structures (Fig. 2C to E), excluded the possibility that a direct physical interaction between NSP4-EGFP and cortical actin was responsible for the recorded changes in cellular morphology (Fig. 1) or increased actin polymerization (Fig. 3). However, for the latter, NSP4-EGFP-controlled changes in intracellular calcium signaling were predicted (Fig. 4). To further address NSP4-EGFP-induced signaling events

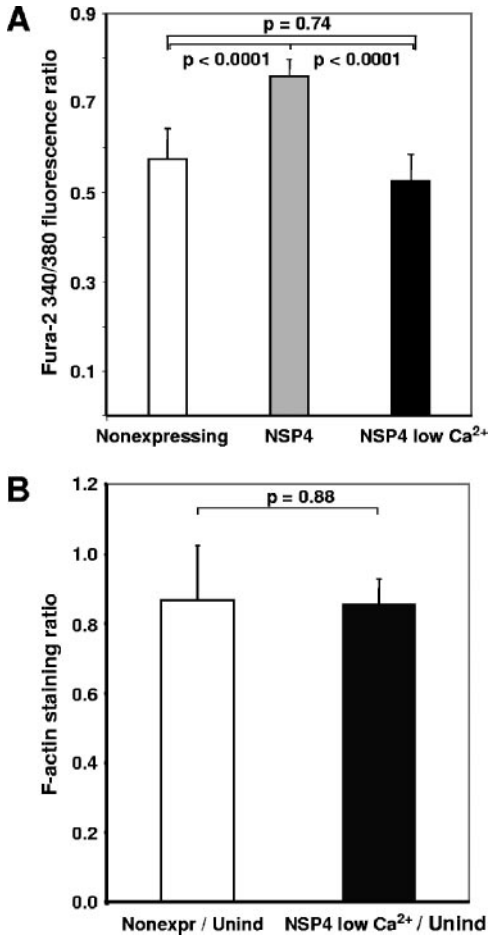

FIG. 4. Increase of F-actin levels in HEK 293 cells expressing NSP4-EGFP is dependent on intracellular calcium levels. Cells were seeded, induced, and incubated in regular or low-calcium medium. Twenty-four hours after seeding/induction, cells were loaded with Fura-2 for measurement of intracellular calcium levels or collected and stained with rhodamine-conjugated phalloidin to measure F-actin content. (A) Fura-2 340/380 fluorescence ratio reflecting intracellular calcium levels in nonexpressing cells ($n = 80$) (white), NSP4-EGFP-expressing cells 24 hpi ($n = 30$) (gray), and NSP4-EGFP-expressing cells grown in a low-calcium medium for 24 h postinduction ($n = 37$) (black). (B) Ratio of F-actin staining for induced nonexpressing cells versus uninduced control cells (white), and for induced NSP4-EGFP-expressing cells grown in low-calcium medium 24 h postinduction versus uninduced controls (black). Data represent six sets of cell populations from two separate experiments. *P* values were calculated using the Student *t* test.

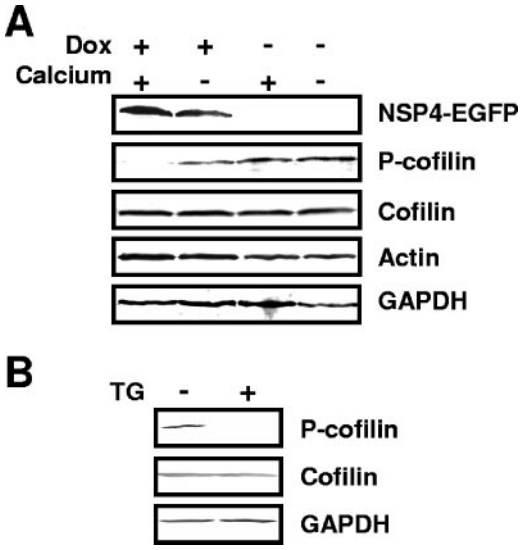

FIG. 5. NSP4-EGFP expression and thapsigargin treatment suppress cofilin phosphorylation in HEK 293 cells as detected by Western blotting. (A) Induced (Dox +) and uninduced (Dox −) HEK 293/NSP4-EGFP cells were grown in the regular (Calcium +) or low-calcium (Calcium −) medium. Cells were harvested 24 to 48 h postinduction. (B) HEK 293 cells were grown in regular medium and, 8 h prior to harvesting, were treated with 200 nM thapsigargin. Whole-cell lysates were separated by SDS-PAGE, and the indicated proteins were detected by Western blotting with GAPDH as the loading control.

linked to these changes, we looked at the primary signaling pathways known to regulate actin polymerization and cellular actin redistribution. Actin homeostasis in all cells is regulated by a number of major signaling GTPases: Rho, Rac, and CDC-42 (41). These enzymes regulate key changes in actin-mediated plasma membrane turnover, leading to morphological shape changes in quiescent, dividing, and locomoting cells (see Discussion). To detect differences in the activation state of each enzyme, we used EZ-Detect Rho, Rac, and CDC-42 activation kits (Pierce Biotechnology, Inc., Rockford, IL) to pull down active GTP-bound GTPases from NSP4-EGFP-expressing (doxycycline-induced) and non-NSP4-EGFP-expressing (uninduced) cell lysates. Although each enzyme was found, we failed to observe any difference in their activation status following NSP4-EGFP induction (data not shown).

The failure to detect involvement for any of these three signaling GTPases in NSP4-induced changes in actin homeostasis may reflect a low signal-to-noise ratio for immunodetection in our cell system because of low levels of endogenous enzymes. Alternatively, it also predicted that NSP4-signaling events linked to subcortical actin reorganization distal to these signaling molecules may be more important. To test the latter hypothesis, calcium-regulated proteins proximal to actin polymerization but distal to the signaling effects of the GTPases studied above were investigated further.

One possible candidate was the actin-remodeling protein cofilin, whose actin turnover activity is regulated by phosphorylation/dephosphorylation on Ser3 (1, 38). Elevated intracellular calcium levels have been shown to activate cofilin by decreasing cofilin phosphorylation by two mechanisms: via downregulation of LIM kinase (46) and by activation of Slingshot phosphatase (47). Further, the expression of the caged phosphorylation-resistant and thus inducibly active cofilin mutant S3A has been shown to increase F-actin content by 40% (a 1.4-fold increase) in MLTn3 cells (23). We tested the hypothesis that lowered cellular phosphocofilin content would accompany the observed changes in subcortical actin polymerization in NSP4-EGFP-expressing cells because of an NSP4-induced elevation of intracellular calcium levels.

Cellular lysates prepared from paired NSP4-EGFP-expressing (doxycycline-induced) and nonexpressing (uninduced) HEK 293 cells were probed by Western blotting for total cellular cofilin and phosphocofilin levels (Fig. 5A). In agreement

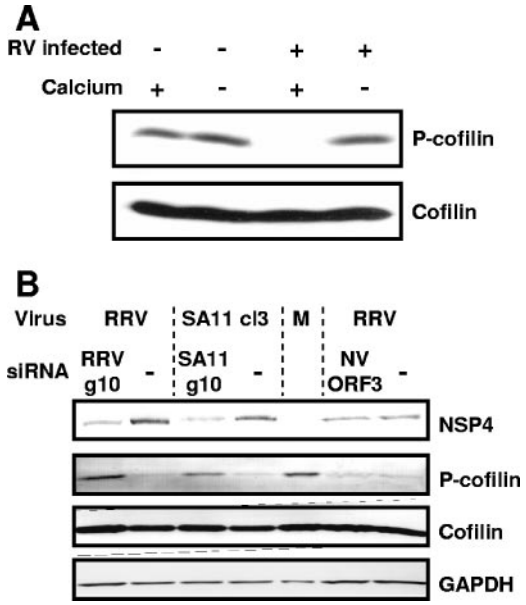

FIG. 6. Cofilin phosphorylation is also suppressed in rotavirus-infected MA104 cells. (A) Total cofilin and phosphocofilin were detected by Western blotting in whole-cell lysates of rotavirus SA114F-infected (RV infected +) and uninfected (RV infected −) MA104 cells grown in regular (Calcium +) or low-calcium (Calcium −) medium. (B) Rotavirus strain RRV and SA11-infected MA104 cells transfected with RRV and an SA11-specific siRNA (RRV g10 and SA11 g10) to suppress NSP4 expression. A Norwalk virus ORF3 siRNA was used as a negative control.

with our hypothesis, the amount of phosphorylated cofilin detected in NSP4-EGFP-expressing cells grown in regular culture medium (with doxycycline and calcium) was significantly lower (almost undetectable) than the amount of phosphorylated cofilin detected in uninduced cells (without doxycycline) grown in either regular (with calcium) or calcium-free culture medium. Densitometric analysis revealed that levels of phosphocofilin relative to total cellular cofilin were more than 40-fold lower in NSP4-EGFP-expressing cells (with doxycycline and calcium) than in uninduced cells (with calcium but without doxycycline) and more than 25-fold lower than in NSP4-EGFP-expressing cells cultured in low-calcium medium to normalize intracellular calcium levels (with doxycycline but without calcium) (5). Corroborating these findings, the level of phosphocofilin was also significantly decreased in HEK 293 cells transiently expressing an NSP4-DsRed chimeric fusion protein, but not red fluorescent protein (DsRed) alone (data not shown). To further confirm that elevation of intracellular calcium levels affects the phosphorylation status of cofilin, we treated HEK 293 cells with the calcium-mobilizing agent thapsigargin. Treatment of cells with 200 nM thapsigargin for 8 h was shown previously to induce an endoplasmic reticulum stress response due to an alteration of calcium homeostasis similar to that induced by NSP4 (48). Thapsigargin treatment decreased cofilin phosphorylation in HEK 293 cells (Fig. 5B). These findings confirmed that NSP4-EGFP expression altered cellular cofilin phosphorylation levels and hence that the activation status of cofilin through signaling pathways linked to intracellular calcium homeostasis.

Levels of the phosphorylated form of cofilin are decreased in rotavirus-infected cells. To validate the data obtained with our stable NSP4-EGFP-expressing cell line and with transiently transfected cells, we next analyzed by Western blotting the phosphorylation state of cofilin in MA104 cells infected with both the neuraminidase-sensitive rotavirus strain SA11 (Fig. 6A) and the neuraminidase-resistant rotavirus strain PA169 (data not shown). In both instances, almost undetectable levels of phosphocofilin were observed in rotavirus-infected cells grown in regular medium (with calcium) (Fig. 6A). In agreement with the results obtained following inducible NSP4-EGFP expression (Fig. 5A), phosphocofilin was detected in rotavirus-infected cells grown in low-extracellular-calcium medium to normalize the effects of viral NSP4 production on intracellular calcium levels (Fig. 6A). To further prove the involvement of NSP4 in the observed suppression of phosphocofilin in rotavirus-infected cells, we used siRNA technology to interfere with NSP4 expression in infected cells. As expected, NSP4 siRNA reduced NSP4 expression and increased phosphocofilin levels in rotavirus-infected cells (Fig. 6B), while a control Norwalk virus ORF3 siRNA had no effect. These findings confirmed that the phosphorylation status of cofilin is similarly affected by intracellular NSP4 expression in transfected and rotavirus-infected cells and is related to calcium homeostasis.

DISCUSSION

The rotavirus enterotoxin NSP4 is a pleiotropic protein involved in virus pathogenesis and morphogenesis (3, 19). To date, most studies of the role of NSP4 in virus pathogenesis have focused on extracellular NSP4, due to its ability to elevate intracellular calcium levels through activation of PLC (4, 18). In the studies reported here, we aimed to elucidate whether there is a possible role of intracellular NSP4, shown to chronically elevate intracellular calcium levels (6), in rotavirus pathogenesis. Here we report that NSP4-EGFP expression in HEK 293 cells causes changes in cellular morphology and the organization of the cellular subcortical actin network. HEK 293 cells grown on tissue culture plates into densely packed multicell layers exhibit few cellular protrusions. However, when NSP4-EGFP is expressed in the confluent cells, long cellular protrusions reminiscent of cells growing at low density were observed. These projections characteristically contain large areas of subcortical actin packed into "finger-like" plasma membrane protrusions. This effect, together with the partial resistance of NSP4-EGFP-expressing cells to the cellular actin cytoskeleton-disrupting agent cytochalasin D, points to the possibility that NSP4 intracellular signaling remodels the actin network during viral infection and mucosal pathogenesis. NSP4-EGFP-expressing cells and rotavirus-infected cells also contained increased cellular F-actin levels, strongly suggesting that changes in subcortical actin polymerization (41) underlie this altered morphology and are regulated by NSP4-stimulated signaling pathways. As we show in the present report, NSP4-induced increased actin polymerization is a calcium-regulated process linked to changes in the activation status of the actin-remodeling protein cofilin in both NSP4-expressing and rotavirus-infected cells. When cells were maintained under conditions that normalized their intracellular calcium levels (5),

both F-actin and phosphocofilin levels were comparable to those in control cells.

Cofilin is a highly conserved, actin dynamics-regulating protein, ubiquitously expressed in all eukaryotes, and is directly involved in actin polymerization and the formation of protrusions (17). Expression of the inducibly active cofilin mutant S3A leads to a 1.4-fold increase in F-actin content, while, surprisingly, the inactive mutant has no effect on F-actin content in MLTn3 rat mammary adenocarcinoma cells (23). Two functions of cofilin are involved in actin dynamics: severing of actin filaments to generate more barbed ends (13) and actin depolymerization at the pointed ends (11). The interplay of those two functions may differ by cell type. More recent data support the notion that the severing activity of cofilin amplifies the nucleation ability of the Arp2/3 complex, resulting in increased actin polymerization through a synergy between the two (17, 26). This can explain the increased F-actin content in NSP4-EGFP-expressing cells described in this paper. Cytochalasin D interferes with actin organization by binding to the barbed ends and thus releasing actin from the periplasmic region, resulting in the formation of F-actin foci (14). The increased number of barbed ends in NSP4-EGFP-expressing cells during cofilin-induced peripheral subcortical network actin remodeling may explain the resistance of NSP4-EGFP-expressing cells to cytochalasin D.

Cofilin activity is regulated by a reversible phosphorylation of the Ser3 residue, and it is under strict spatial control via specific localization of kinases and phosphatases (37). At least one of the kinases involved in cofilin regulation, LIM kinase 1 (LIMK1), has been shown to be transcriptionally downregulated by calcineurin in response to calcium influx causing elevation of intracellular calcium levels (46). Conversely, the cofilin phosphatase Slingshot is known to be activated by elevated intracellular calcium levels via calcineurin-induced dephosphorylation (47). However, the recently identified downregulation of LIMK1 activity by Slingshot (43) complicates the delineation of which one of these calcium-regulated effectors of cofilin plays the lead role in changing cofilin's phosphorylation status in NSP4-EGFP-expressing cells. The paucity of readily available assays to measure the activity of either enzyme is a technical barrier which requires future studies. From the results presented here, it is intriguing to speculate that through chronic PLC-independent intracellular calcium mobilization (6), NSP4 affects the phosphorylation level of cofilin, and thus its cofilin activation status via a direct calcineurin-mediated regulation of cofilin kinase and/or phosphatase, without the need to engage Rho, Rac, or CDC-42 upstream in the signaling pathways.

How do NSP4-mediated changes in subcortical actin benefit the virus? Rotavirus infection leads to a calcium-dependent loss of microvillar actin and a disorganization of microtubules in infected polarized (differentiated) Caco-2 cells (9, 10). Since the HEK 293-derived cells used in our study are rapidly growing transformed embryonic cells, which are relatively undifferentiated and nonpolarized, they lack a brush border (apical surface) and are thus a model for the epithelial basolateral membrane (32). The observed changes in actin dynamics following NSP4-EGFP expression described here are, therefore, best extrapolated to NSP4-signaling events occurring at the basolateral membrane of virus-infected small intestinal epithelial cells. We speculate that virus infection leads to stiffening of the basolateral subcortical network, providing an additional fence across this membrane, possibly directing nascent viral release across the apical membrane into the intestinal lumen.

Gardet et al. (22) recently described a rotavirus VP4 interaction with actin in EGFP-VP4-transfected and rotavirus-infected cells causing dissolution of apical microvilli, in agreement with an earlier report of loss of apical microvillar actin in rotavirus-infected polarized cells (9). Our results describe an effect of NSP4 expression on subcortical actin organization, namely, increased polymerization. Thus, it appears that the VP4 and NSP4 rotavirus proteins elicit geographically separate but synergistic functions related to polarized virus release: weakening of the apical membrane actin network by direct interaction with VP4 (22) and stiffening of the basolateral actin network mediated by NSP4-induced calcium-dependent activation of cofilin.

Changes in subcortical actin dynamics and dysregulation of cofilin can affect endo- and exocytosis, receptor internalization, channel activity, and ion gradients (29, 30, 36, 42), thus directly contributing to rotavirus pathogenesis. Translocation of inactive/dephosphorylated cofilin into mitochondria has been shown to be directly linked to apoptosis (12, 14). Although we did not observe increased annexin V staining in NSP4-EGFP-expressing cells (data not shown), the effect of NSP4 on apoptotic signaling should be further investigated. Future studies of the effects of NSP4 on actin network organization and their relationship to rotavirus infection and pathogenesis should be carried out on NSP4-expressing polarized cell lines when they become available.

ACKNOWLEDGMENTS

This work was supported in part by Public Health Service grants RO1 DK30144, RO1 DK59550, and P30 DK056338 that support the Texas Gulf Coast Digestive Disease Center.

REFERENCES

1. **Arber, S., F. A. Barbayannis, H. Hanser, C. Schneider, C. A. Stanyon, O. Bernard, and P. Caroni.** 1998. Regulation of actin dynamics through phosphorylation of cofilin by LIM-kinase. Nature **393:**805–809.
2. **Azevedo, A. S., L. Yuan, K. I. Jeong, A. Gonzalez, T. V. Nguyen, S. Pouly, M. Gochnauer, W. Zhang, A. Azevedo, and L. J. Saif.** 2005. Viremia and nasal and rectal shedding of rotavirus in gnotobiotic pigs inoculated with Wa human rotavirus. J. Virol. **79:**5428–5436.
3. **Ball, J. M., D. M. Mitchell, T. F. Gibbons, and R. D. Parr.** 2005. Rotavirus NSP4: a multifunctional viral enterotoxin. Viral Immunol. **18:**27–40.
4. **Ball, J. M., P. Tian, C. Q.-Y. Zeng, A. P. Morris, and M. K. Estes.** 1996. Age-dependent diarrhea induced by a rotaviral nonstructural glycoprotein. Science **272:**101–104.
5. **Berkova, Z., S. E. Crawford, G. Trugnan, T. Yoshimori, A. P. Morris, and M. K. Estes.** 2006. Rotavirus NSP4 induces a novel vesicular compartment regulated by calcium and associated with viroplasms. J. Virol. **80:**6061–6071.
6. **Berkova, Z., A. P. Morris, and M. K. Estes.** 2003. Cytoplasmic calcium measurement in rotavirus enterotoxin-enhanced green fluorescent protein (NSP4-EGFP) expressing cells loaded with Fura-2. Cell Calcium **34:**55–68.
7. **Blutt, S. E., M. Fenaux, K. L. Warfield, H. B. Greenberg, and M. E. Conner.** 2006. Active viremia in rotavirus-infected mice. J. Virol. **80:**6702–6705.
8. **Blutt, S. E., C. D. Kirkwood, V. Parreno, K. L. Warfield, M. Ciarlet, M. K. Estes, K. Bok, R. F. Bishop, and M. E. Conner.** 2003. Rotavirus antigenaemia and viraemia: a common event? Lancet **362:**1445–1449.
9. **Brunet, J. P., J. Cotte-Laffitte, C. Linxe, A. M. Quero, M. Geniteau-Legendre, and A. Servin.** 2000. Rotavirus infection induces an increase in intracellular calcium concentration in human intestinal epithelial cells: role in microvillar actin alteration. J. Virol. **74:**2323–2332.
10. **Brunet, J. P., N. Jourdan, J. Cotte-Laffite, C. Linxe, M. Geniteau-Legendre, A. Servin, and A. M. Quero.** 2000. Rotavirus infection induces cytoskeleton disorganization in human intestinal epithelial cells: implication of an increase in intracellular calcium concentration. J. Virol. **74:**10801–10806.
11. **Carlier, M. F., V. Laurent, J. Santolini, R. Melki, D. Didry, G. X. Xia, Y.**

Hong, N. H. Chua, and D. Pantaloni. 1997. Actin depolymerizing factor (ADF/cofilin) enhances the rate of filament turnover: implication in actin-based motility. J. Cell Biol. **136:**1307–1322.
12. **Chua, B. T., C. Volbracht, K. O. Tan, R. Li, V. C. Yu, and P. Li.** 2003. Mitochondrial translocation of cofilin is an early step in apoptosis induction. Nat. Cell Biol. **5:**1083–1089.
13. **Condeelis, J.** 2001. How is actin polymerization nucleated in vivo? Trends Cell Biol. **11:**288–293.
14. **Cooper, J. A.** 1987. Effects of cytochalasin and phalloidin on actin. J. Cell Biol. **105:**1473–1478.
15. **Crawford, S. E., D. G. Patel, E. Cheng, Z. Berkova, J. M. Hyser, M. Ciarlet, M. J. Finegold, M. E. Conner, and M. K. Estes.** 2006. Rotavirus viremia and extraintestinal viral infection in the neonatal rat model. J. Virol. **80:**4820–4832.
16. **Davidson, G. P., R. F. Bishop, R. R. Townley, and I. H. Holmes.** 1975. Importance of a new virus in acute sporadic enteritis in children. Lancet **i:**242–246.
17. **DesMarais, V., F. Macaluso, J. Condeelis, and M. Bailly.** 2004. Synergistic interaction between the Arp2/3 complex and cofilin drives stimulated lamellipod extension. J. Cell Sci. **117:**3499–3510.
18. **Dong, Y., C. Q.-Y. Zeng, J. M. Ball, M. K. Estes, and A. P. Morris.** 1997. The rotavirus enterotoxin NSP4 mobilizes intracellular calcium in human intestinal cells by stimulating phospholipase C-mediated inositol 1,4,5-trisphosphate production. Proc. Natl. Acad. Sci. USA **94:**3960–3965.
19. **Estes, M. K., G. Kang, C. Q.-T. Zeng, S. E. Crawford, and M. Ciarlet.** 2001. Pathogenesis of rotavirus gastroenteritis, p. 82–100. *In* D. Chadwick and J. A. Goode (ed.), Gastroenteritis viruses. Novartis Foundation Symposium 238. John Wiley & Sons Ltd., Chichester, United Kingdom.
20. **Faix, J., and K. Rottner.** 2006. The making of filopodia. Curr. Opin. Cell Biol. **18:**18–25.
21. **Fischer, T. K., D. Ashley, T. Kerin, E. Reynolds-Hedmann, J. Gentsch, M. A. Widdowson, L. Westerman, N. Puhr, R. M. Turcios, and R. I. Glass.** 2005. Rotavirus antigenemia in patients with acute gastroenteritis. J. Infect. Dis. **192:**913–919.
22. **Gardet, A., M. Breton, P. Fontages, G. Trugnan, and S. Chwetzoff.** 2006. Rotavirus spike protein VP4 binds to and remodels actin bundles of the epithelial brush order into actin bodies. J. Virol. **80:**3947–3956.
23. **Ghosh, M., X. Y. Song, G. Mouneimne, M. Sidani, D. S. Lawrence, and J. S. Condeelis.** 2004. Cofilin promotes actin polymerization and defines the direction of cell motility. Science **304:**743–746.
24. **Hayot, C., O. Debeir, P. Van Ham, M. Van Damme, R. Kiss, and C. Decaestecker.** 2006. Characterization of the activities of actin-affecting drugs on tumor cell migration. Toxicol. Appl. Pharmacol. **211:**30–40.
25. **Holmes, I. H.** 1979. Viral gastroenteritis. Prog. Med. Virol. **25:**1–36.
26. **Ichetovkin, I., W. Grant, and J. Condeelis.** 2002. Cofilin produces newly polymerized actin filaments that are preferred for dendritic nucleation by the Arp2/3 complex. Curr. Biol. **12:**79–84.
27. **Jourdan, N., J. P. Brunet, C. Sapin, A. Blais, J. Cotte-Laffitte, F. Forestier, A. M. Quero, G. Trugnan, and A. L. Servin.** 1998. Rotavirus infection reduces sucrase-isomaltase expression in human intestinal epithelial cells by perturbing protein targeting and organization of microvillar cytoskeleton. J. Virol. **72:**7228–7236.
28. **Ku, N. O., X. J. Zhou, D. M. Toivola, and M. B. Omary.** 1999. The cytoskeleton of digestive epithelia in health and disease. Am. J. Physiol. **277:**G1108–G1137.
29. **Lee, K., J. H. Jung, M. Kim, and G. Guidotti.** 2001. Interaction of the alpha subunit of Na, K-ATPase with cofilin. Biochem. J. **353:**377–385.
30. **Lockwich, T., B. B. Singh, X. B. Liu, and I. S. Ambudkar.** 2001. Stabilization of cortical actin induces internalization of transient receptor potential 3 (Trp3)-associated caveolar Ca^{2+} signaling complex and loss of Ca^{2+} influx without disruption of Trp3-inositol trisphosphate receptor association. J. Biol. Chem. **276:**42401–42408.
31. **Lopez, T., M. Camacho, M. Zayas, R. Najera, R. Sanchez, C. F. Arias, and S. Lopez.** 2005. Silencing the morphogenesis of rotavirus. J. Virol. **79:**184–192.
32. **Morris, A. P., and R. A. Frizzell.** 1994. Vesicle targeting and ion secretion in epithelial cells: implications for cystic fibrosis. Annu. Rev. Physiol. **56:**371–397.
33. **Morris, A. P., K. L. Kirk, and R. A. Frizzell.** 1990. Simultaneous analysis of cell Ca^{2+} and Ca^{2+}-stimulated chloride conductance in colonic epithelial cells (HT-29). Cell Regul. **1:**951–963.
34. **Mossel, E. C., and R. F. Ramig.** 2002. Rotavirus genome segment 7 (NSP3) is a determinant of extraintestinal spread in the neonatal mouse. J. Virol. **76:**6502–6509.
35. **Mossel, E. C., and R. F. Ramig.** 2003. A lymphatic mechanism of rotavirus extraintestinal spread in the neonatal mouse. J. Virol. **77:**12352–12356.
36. **Muallem, S., K. Kwiatkowska, X. Xu, and H. L. Yin.** 1995. Actin filament disassembly is a sufficient final trigger for exocytosis in nonexcitable cells. J. Cell Biol. **128:**589–598.
37. **Nishita, M., C. Tomizawa, M. Yamamoto, Y. Horita, K. Ohashi, and K. Mizuno.** 2005. Spatial and temporal regulation of cofilin activity by LIM kinase and slingshot is critical for directional cell migration. J. Cell Biol. **171:**349–359.
38. **Niwa, R., K. Nagata-Ohashi, M. Takeichi, K. Mizuno, and T. Uemura.** 2002. Control of actin reorganization by slingshot, a family of phosphatases that dephosphorylate ADF/cofilin. Cell **108:**233–246.
39. **Obert, G., I. Peiffer, and A. L. Servin.** 2000. Rotavirus-induced structural and functional alterations in tight junctions of polarized intestinal Caco-2 cell monolayers. J. Virol. **74:**4645–4651.
40. **Parashar, U. D., E. G. Hummelman, J. S. Bresee, M. A. Miller, and R. I. Glass.** 2003. Global illness and deaths caused by rotavirus disease in children. Emerg. Infect. Dis. **9:**565–572.
41. **Small, J. V., K. Rottner, and I. Kaverina.** 1999. Functional design in the actin cytoskeleton. Curr. Opin. Cell Biol. **11:**54–60.
42. **Song, J. C., B. J. Hrnjez, O. C. Farokhzad, and J. B. Matthews.** 1999. PKC-epsilon regulates basolateral endocytosis in human T84 intestinal epithelia: role of F-actin and MARCKS. Am. J. Physiol. **277:**C1239–C1249.
43. **Soosairajah, J., S. Maiti, O. Wiggan, P. Sarmiere, N. Moussi, B. Sarcevic, R. Sampath, J. R. Bamburg, and O. Bernard.** 2005. Interplay between components of a novel LIM kinase-slingshot phosphatase complex regulates cofilin. EMBO J. **24:**473–486.
44. **Tafazoli, F., C. Q.-Y. Zeng, M. K. Estes, K. E. Magnusson, and L. Svensson.** 2001. The NSP4 enterotoxin of rotavirus induces paracellular leakage in polarized epithelial cells. J. Virol. **75:**1540–1546.
45. **Tian, P., A. Ottaiano, P. A. Reilly, S. Udem, and T. Zamb.** 2000. The authentic sequence of rotavirus SA11 nonstructural protein NSP4. Virus Res. **66:**117–122.
46. **Tojima, T., M. Takahashi, and E. Ito.** 2003. Dual regulation of LIM kinase 1 expression by cyclic AMP and calcium determines cofilin phosphorylation states during neuritogenesis in NG108-15 cells. Brain Res. **985:**43–55.
47. **Wang, Y., F. Shibasaki, and K. Mizuno.** 2005. Calcium signal-induced cofilin dephosphorylation is mediated by slingshot via calcineurin. J. Biol. Chem. **280:**12683–12689.
48. **Xu, A., A. R. Bellamy, and J. A. Taylor.** 1999. Expression of translationally controlled tumour protein is regulated by calcium at both the transcriptional and post-transcriptional level. Biochem. J. **342:**683–689.
49. **Zhang, M., C. Q.-Y. Zeng, A. P. Morris, and M. K. Estes.** 2000. A functional NSP4 enterotoxin peptide secreted from rotavirus-infected cells. J. Virol. **74:**11663–11670.
50. **Zhao, W., M. J. Xia, T. Bridges-Malveo, M. Cantu, M. M. McNeal, A. H. Choi, R. L. Ward, and K. Sestak.** 2005. Evaluation of rotavirus dsRNA load in specimens and body fluids from experimentally infected juvenile macaques by real-time PCR. Virology **341:**248–256.